Extended Abstracts of the 2009 International Conference on Solid State Devices and Materials, Sendai, 2009, pp36-37

B-1-1(Invited)

Microscopic Characterization of Devices by Scanning Transmission Electron Microscopy: From Single Atom Imaging to Macroscopic Properties

S.J. Pennycook[1,2], K. van Benthem[1,3], A.G. Marinopoulos[1,4] and S.T. Pantelides[2,1]

[1]Materials Science and Technology Division, Oak Ridge National Laboratory, Oak Ridge, TN 37831-6071, USA
Phone: +1-865-574-5504 E-mail: pennycooksj@ornl.gov
[2]Department of Physics and Astronomy, Vanderbilt University, Nashville, TN 37235, USA,
[3]Dept. for Chemical Engineering and Materials Science, University of California, Davis, CA 95616, USA
[4]Dept. of Physics, University of Coimbra, Coimbra, Portugal

1. Introduction

The aberration-corrected scanning transmission electron microscope (STEM) provides a new level of sensitivity for analyzing semiconductor device structures, and when combined with density functional theory, is able to provide a microscopic interpretation of macroscopic device properties. Sub-Ångström probes are now routinely available [1-3], and provide not only improved resolution, but greatly increased sensitivity to individual atoms. Individual high atomic number atoms been imaged with a high angle annular dark field (HAADF) detector [3-5], as shown in Fig. 1. The atoms are not visible in bright field image obtained simultaneously. Individual dopant atoms have also been spectroscopically identified inside their bulk environment [6]. Furthermore, the depth of field of the aberration-corrected STEM is just a few nanometers, so atoms well-separated in depth can be located to high precision.

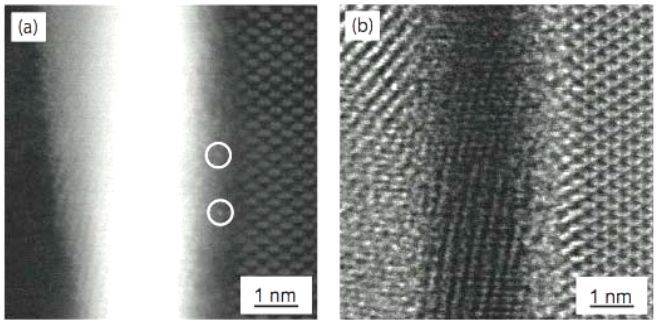

Fig. 1 (a) HAADF image, (b) bright field image of a $HfO_2/SiO_2/Si$ high-K dielectric device structure. Circles mark bright spots representing individual Hf atoms inside the SiO_2. Results obtained with a VG Microscopes HB603U with Nion aberration corrector at 300 kV, reproduced from [7].

2. Analysis of $HfO_2/SiO_2/Si$ High-k Dielectric

Single Hf atoms were observed within the nanometer thick SiO_2 interlayer between a HfO_2 high-*k* dielectric and the Si substrate [8,9]. Figure 2 shows a focal series of images in which the atom circled can be located in depth to better than 1 nm. A total of 65 atoms were detected in the entire focal series and each of their 3D coordinates could therefore be determined. Their average density is 1.4 nm^{-3} giving an average separation of only 0.7 nm.

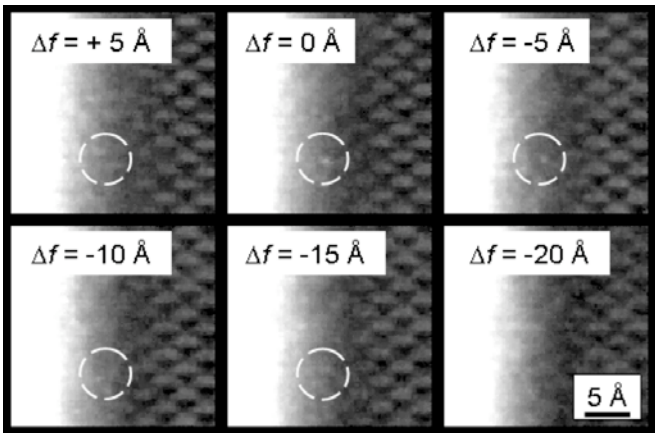

Fig. 2 A focal series of HAADF images showing a Hf atom coming in and out of focus. Reproduced from [8].

Strikingly, no Hf atoms were found in contact with the Si substrate, and they exhibited preferred distances from the interface. First-principles density-functional calculations reveal the origin of this behavior is the increasing order and reduced ring size in the SiO_2 layer as the interface is approached, which makes it energetically unfavorable for Hf to approach the interface, see Fig. 3 [10].

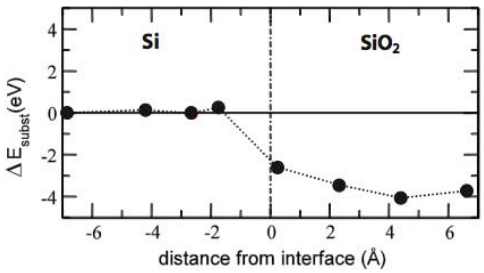

Fig. 3 Plot showing the formation energy for substitutional Hf atoms across the interface. Hf atoms at the interface are 1.4 eV higher in energy than those in the center of the oxide, explaining why no Hf atoms were found at the interface. Adapted from [10].

Nevertheless, localized states are created within the Si band gap, as shown in Fig. 4. These states may mediate leakage at the high densities observed in this case. In addition, they may affect channel mobilities. Calculations of scattering rates are consistent with measured mobility values [11].

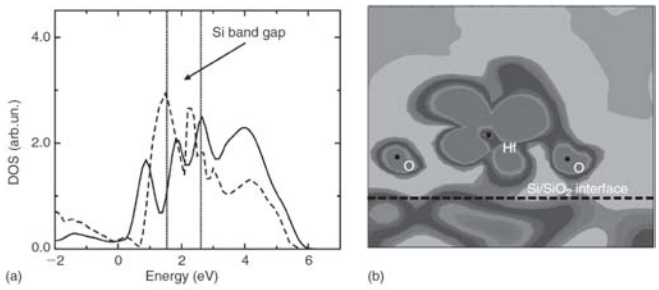

Fig. 4 (a) Densities of states around two interstitial Hf atoms overlap the Si band gap. (b) Plot of the Hf 4d localized state, and the wave function of the bottom of the Si conduction band, showing a significant extent. Adapted from [12].

Electron energy loss spectroscopy has detected the presence of localized states in this region of the device, as shown in Fig. 5. Analysis of the fine structure indicates the formation of oxygen vacancies during rapid thermal annealing [13].

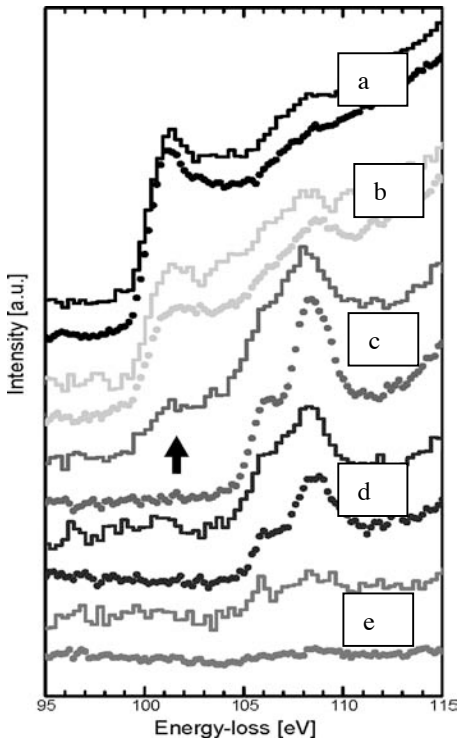

Fig. 5 Averaged EELS absorption edges for the as-deposited (*dotted lines*) and the annealed sample (*solid lines*) in (a) the Si substrate (b) at the SiO_2/Si interface; purple in the center of the SiO_2 film; blue at the HfO_2/SiO_2 interface; and brown in the HfO_2 film. The arrow marks localized states in the SiO_2 after annealing. Data adapted from [13].

3. Conclusions

The combination of atomic-scale 3D structural and electronic characterization available with a modern aberration-corrected STEM, combined with first principles calculations offers the potential to unravel the true microscopic origins of macroscopic device properties. For additional discussion readers are referred to recent review articles [14,15].

References

[1] P. D. Nellist et al., Science **305** (2004) 1741.

[2] H. Sawada, F. Hosokawai, T. Kaneyama, T. Ishizawa, M. Terao, M. Kawazoe, T. Sannomiya, T. Tomita, Y. Kondo, T. Tanaka, Y. Oshima, Y. Tanishiro, N. Yamamoto and K. Takayanagi, Jpn. J. Appl. Phys. **46** (2007) L568.

[3] C. Kisielowski, B. Freitag, M. Bischoff, H. van Lin, S. Lazar, G. Knippels, P. Tiemeijer, M. van der Stam, S. von Harrach, M. Stekelenburg, M. Haider, S. Uhlemann, H. Muller, P. Hartel, B. Kabius, D. Miller, I. Petrov, E. A. Olson, T. Donchev, E. A. Kenik, A. R. Lupini, J. Bentley, S. J. Pennycook, I. M. Anderson, A. M. Minor, A. K. Schmid, T. Duden, V. Radmilovic, Q. M. Ramasse, M. Watanabe, R. Erni, E. A. Stach, P. Denes and U. Dahmen, Microscopy and Microanalysis **14**, 469 (2008).

[4] S. Wang, A. Y. Borisevich, S. N. Rashkeev, M. V. Glazoff, K. Sohlberg, S. J. Pennycook and S. T. Pantelides, Nature Materials **3** (2004) 143.

[5] A. Y. Borisevich, A. R. Lupini and S. J. Pennycook, Proc. Natl. Acad. Sci. USA, **103** (2006) 3044.

[6] M. Varela, S. D. Findlay, A. R. Lupini, H. M. Christen, A. Y. Borisevich, N. Dellby, O. L. Krivanek, P. D. Nellist, M. P. Oxley, L. J. Allen and S. J. Pennycook, Phys. Rev. Lett., **92** (2004) 095502,

[7] S. N. Rashkeev, K. van Benthem, S. T. Pantelides and S. J. Pennycook, Microelectron. Eng., **80** (2005) 416.

[8] K. van Benthem, A. R. Lupini, M. Kim, H. S. Baik, S. Doh, J. H. Lee, M. P. Oxley, S. D. Findlay, L. J. Allen, J. T. Luck and S. J. Pennycook, Appl. Phys. Lett., **87** (2005) 034104.

[9] K. van Benthem, A. R. Lupini, M. P. Oxley, S. D. Findlay, L. J. Allen and S. J. Pennycook, Ultramicroscopy **106**, (2006) 1062.

[10] A. G. Marinopoulos, K. van Benthem, S. N. Rashkeev, S. J. Pennycook and S. T. Pantelides, Phys. Rev. B **77**, (2008) 195317.

[11] M. H. Evans, M. Caussanel, R. D. Schrimpf and S. T. Pantelides, IEDM Tech. Digest (2005) 597.

[12] S. T. Pantelides, M. H. Evans, D. M. Fleetwood, E. P. Gusev, J. D. Joannopoulos, Z. Lu, S. N. Rashkeev, R. D. Schrimpf, L. Tsetseris, K. van Benthem, X.-G. Zhang and X. J. Zhou, in *Proceedings of the NATO Advanced Research Workshop on Defects in High-K Dielectrics and Nano-Electronic Semiconductor Devices,* Springer, (2005) 189.

[13] G. Bersuker, C. S. Park, J. Barnett, P. S. Lysaght, P. D. Kirsch, C. D. Young, R. Choi, B. H. Lee, B. Foran, K. van Benthem, S. J. Pennycook, P. M. Lenahan and J. T. Ryan, J. Appl. Phys. **100**, (2006) 094108.

[14] K. van Benthem and S. J. Pennycook, Appl. Phys. A **96**, (2009) 161.

[15] S. J. Pennycook, M. F. Chisholm, K. van Benthem, A. G. Marinopoulos, and S. T. Pantelides, in *Defects in Microelectronic Materials and Devices*, edited by D. M. Fleetwood, R. D. Shrimpf and S. T. Pantelides (CRC Press, Boca Raton) 2008 259.

[16] This work was supported by DOE Basic Energy Sciences, Division of Materials Science and Engineering, the ORNL LDRD program and by appointment (KvB) to the ORNL Postdoctoral Research Program administered jointly by ORNL and ORISE.